

Bock, S. (2014). Numerical modelling of a void behind shaft lining using FDM with a concrete spalling algorithm. *Journal of Sustainable Mining*, 13(2), 14–21.
doi:10.7424/jsm140203

ORIGINAL PAPER

Received: 11 April 2014 | Revised: 16 June 2014 | Published online: 25 June 2014

NUMERICAL MODELLING OF A VOID BEHIND SHAFT LINING USING FDM WITH A CONCRETE SPALLING ALGORITHM

Sławomir Bock

Department of Extraction Technologies and Mining Support, Central Mining Institute (Katowice, Poland)

Corresponding author: e-mail: sbock@gig.eu, tel.: +48 32 259 24 06, fax: +48 32 258 44 25

ABSTRACT

Purpose	The aim of the research presented in this paper was to determine the impact of voids behind the lining on shaft stability.
Methods	This paper presents an example of extending the FLAC3D with the possibility of the simulation of concrete detachment and separation under specific conditions by means of a developed FISH routine.
Results	The appearance of voids and cavities behind the lining has been repeatedly observed in active shafts in Polish coal mines and can lead to the emergence of tensile forces in the lining. The study included 366 models of shafts using the rock mass properties of typical shale stone, coal, and sandstone found in the Upper Silesian Coal.
Practical implications	The presented concrete spalling algorithm may be used, especially, for the stability evaluation of locally damaged shaft lining or when there is a suspicion of void behind the lining.
Originality/value	An important limitation of all continuous methods is the inability (except when using some additional tools) to simulate the rotations of predefined elements (blocks) and their separation from the rest of the object. The concrete spalling algorithm presented extends the capabilities of FLAC3D with the possibility of simulating the detachment and separation of destroyed lining fragments.

Keywords

mine shaft, shaft lining, numerical modelling, material modelling, FDM

1. INTRODUCTION

Based on the rapid increase in the data processing capacity of computers and the development of increasingly enhanced software for numerical modelling, it seems to be advantageous to use numerical methods to search for design solutions – especially in cases of non-typical mining and geological conditions and in cases that need to consider a large number of factors. The numerical methods currently in use can be classified as follows (Jing, 2003):

- Continuous methods:
 - Finite difference method (FDM),
 - Finite element method (FEM),
 - Boundary element method (BEM).
- Discontinuous methods:
 - Discrete element method (DEM),
 - Discrete fracture network (DFN) methods.
- Hybrid continuous/discontinuous models.

Discontinuous methods are promising for applications in rock and soil mechanics. The main difference between discontinuous and continuous methods is the former's ability to rotate and even detach blocks in the deformation process. Nevertheless, the number of practical applications of discontinuous methods is relatively low, mainly due to the need to select specific rock mass parameters which are difficult to assess under mining and laboratory conditions. In many cases another obstacle is high computational requirements. Due to these disadvantages, FDM, a continuous method, is still successfully used in many aspects of rock mechanics, such as:

- the design of steel arch support in Polish coal mines (Bock, Prusek, & Rotkegel, 2009),
- the design and evaluation of mining shafts (Prusek, Rotkegel, Bock, & Szymała, 2011),
- the estimation of horizontal in situ stress and soil cohesion based on back analysis (Fakhimia, Salehic, & Mojtabai, 2004),

- the analysis of seismic damage to deep underground openings (Genis & Gercek, 2003),
- the analysis of methane emissions and gob gas venthole production (Karacan, Esterhuizen, Schatzel, & Diamond, 2007),
- the design of compensation grouting above shallow tunnels (Wisser, Augarde, & Burd, 2005).

An important advantage of FDM is the relatively simple parameterisation of the model, which allows it to be applied based on results from basic laboratory and underground tests. The use of this method is especially accurate for stability verification of the models in conditions which are undamaged (or slightly damaged). However, in certain cases, there is a need to include the local damage of the structure with the detachment of destroyed parts in the numerical analysis. Such conditions are sometimes observed in the case of old linings of deep mining shafts, where part of the lining is damaged and yet – from the viewpoint of the entire structure – the shaft preserves its stability (Fig. 1).

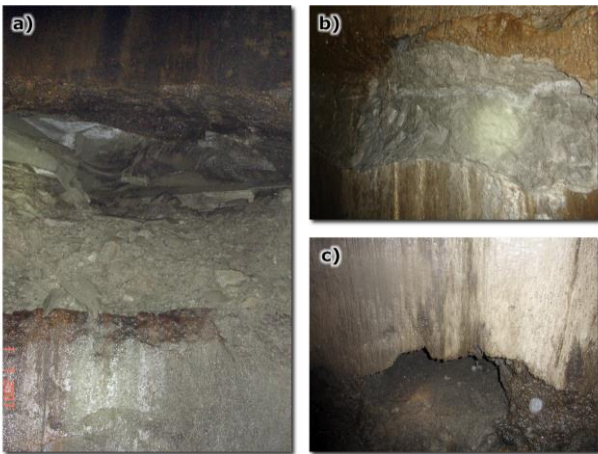


Fig. 1. Examples of deep lining damage: a – very wide and deep lining loss throughout the entire thickness, with rocks visible behind the former lining, b – deep lining damage (to a depth of approximately 20 cm), c – wide and deep lining damage

The technical condition of the lining directly influences the stability of the shaft. The catastrophe at the "Bolesław" shaft in the "Bobrek" colliery of 6 September 1975 confirms this fact. The event was characterised by a very dynamic course and lasted merely 15 hours. First an increased outflow of quicksand from behind the shaft lining at a depth of 24 m was observed during the nightly shaft inspection and a vertical fracture of the lining located below the outflow point. As a result of a concrete gutter element falling out, a 0.8-m long and 0.2-m wide vertical fissure came into existence throughout the whole thickness of the shaft lining. Although provisional packing had been placed in the gap in lining, made of ventilation fabric and planks, a considerable and violent increase of the gap in the lining was observed after a short time, along with an intensive outflow of sand and water. As a result of influence from the water and changes in the load exerted on the shaft lining the latter began breaking over a considerable length. On the western side of the shaft a crater was formed that uncovered foundations of the shaft bank house. After several hours the increasing crater caused the collapse

of the shaft bank building which leaned against the headframe's angled struts, breaking them and causing a collapse of the headframe (Fig. 2).



Fig. 2. View of the collapsed headframe in the "Bolesław" shaft in the "Bobrek" colliery (Lecomte et al., 2012)

The failure of the shaft lining was also the cause of a catastrophe in shaft "V" in the Knurów-Szczygłowice coal mine on the 4th of September 2008. In spite of all the attempts made to repair the lining, the shaft lost its stability. A large crater was formed at the surface that in turn caused damage to the building facilities present in its impact zone (Fig. 3).



Fig. 3. The catastrophe of shaft "V" in the Knurów-Szczygłowice coal mine: a – general view of the scene of the catastrophe from the north (the crater area is marked yellow), b – damaged nearby buildings (Prusek, Bock, Uszko, & Dziura, 2013)

The primary cause of the accident at the shaft was damage (partial loss) of lining at a depth of 61.0–67.0 m. The catastrophe also caused complete destruction of the shaft bank building and headframe which fell over and down into the crater. The crater had a diameter at the ground surface of ca. 60.0 m, a depth of around 11 m and an estimated volume of about 30,000 m³ (Prusek et al., 2013).

The two previous examples show, that the volume of loosened lining leading to a catastrophe is hard to estimate. In the first case the volume of breakage in the lining of only about 0.1 m³ led to the loss of shaft stability. In the second example the shaft collapsed after the loss of a significant volume of lining at a depth of 61–67 m. The amount of critical breakage volume depends inter alia on such factors as the geological and mining conditions, technical state and the load distribution of the lining. The examined technical state of the lining in another shaft of the Upper Silesian Coal Basin confirms this fact. The macroscopic examination of the lining performed by the author showed a great number of lining breakages requiring immediate repair (Table 1). However, despite the large total volume of the breakages (about 13 m³) the shaft maintained its stability.

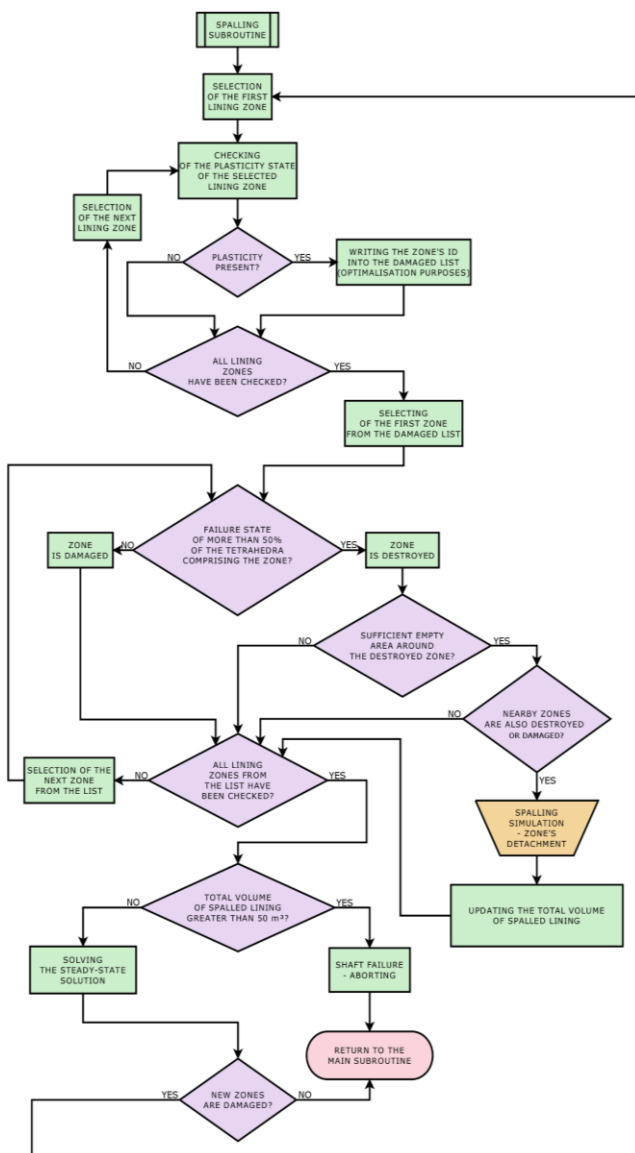
Table 1. Identified losses of the shaft lining

Bunton number	Dimension [m]	Approximate volume [m ³]
128–129	1.0 × 2.5 × 0.3 m	0.8
136	1.5 × 1.0 × 0.3 m	0.5
139	1.5 × 1.0 × 0.3 m	0.5
149	1.5 × 1.0 × 0.3 m	0.5
170	2.5 × 1.5 × 0.3 m	1.1
174	4.0 × 2.0 × 0.4 m	3.2
177	3.0 × 2.5 × 0.5 m	3.8
183	1.5 × 2.5 × 0.3 m	1.1
191	3.0 × 2.0 × 0.5 m	1.5

To improve the numerical analysis, especially in cases where similar damage to that described above, a special algorithm extending the capabilities of FLAC3D code has been developed and implemented using the built-in FISH interpreter.

2. CONCRETE SPALLING ALGORITHM

The developed subroutine continuously analyses the strength factor of particular parts of the lining and allows for their detachment and separation under specific conditions. A diagram of the algorithm is shown in Figure 4.

**Fig. 4.** Diagram of the concrete spalling algorithm

The subroutine developed checks the current plasticity state of a specific group of zones (for example, all zones of the shaft lining). Distinct states of failure (tension and/or shear) were not analysed. If less than 50% of the tetrahedra comprising the zone was in any sort of state of failure, then the zone was marked as damaged (cracked). If at least 50% of the tetrahedra was in a failure state, then the zone was marked as destroyed, and its location was analysed. If the destroyed zone comprised the surface layer of the lining and at least 50% of the adjacent zones around it were also designated as destroyed or damaged, the subroutine executed the spalling simulation, and the selected zone was removed from the model. The assumed value of 50% of failure state of the tetrahedra comprising the zone is resulting from access restrictions of FISH functions – only the two states (below and above 50%) are possible to estimate.

After each execution of the subroutine, the total volume of the removed zones was calculated and compared to the upper limit (default: 50 m³). If the upper limit was exceeded, then the calculation was interrupted and shaft failure was assumed. Otherwise, the equilibrium state was calculated. The subroutine was used until no further spalling simulation was needed after reaching a steady state. In that case, the subroutine exited, and the main program continued. It must be noted, however, that the default upper limit of volume of the removed zone (50 m³) does not indicate the amount of lining required for loss of shaft stability. In all of the analysed numerical models the shaft stability was affected earlier – but it resulted in the expansion of the removed lining zones. Therefore the default upper limit equal to 50 m³ was introduced to prevent unnecessary further computations.

3. VERIFICATION OF CONCRETE SPALLING ALGORITHM

The verification of the spalling algorithm was performed based on the examination of the void in one of the shafts of the Upper Silesian Coal Basin. The shaft, with a diameter of 7.5 m, was sunk in 1972–1974. The void was located at a depth of about 90 m. The void's examination was carried out by means of macroscopic observations of the lining and an optical tool for borehole inspection. The macroscopic inspections of the shaft in area of the void showed a dry lining, without visible water leakages, generally with good conditions. However, close up inspections showed that the concrete could be removed by bare hands in certain regions of the lining. In the area of the void only a small opening in the lining is visible (Fig. 5a). However, further optical (introsopic) inspections confirmed the presence of the void with dimensions of approximately 0.7 × 0.8 × 0.9 m. The presence of corrosion products in the roof of the void (Fig. 5b) indicates that it was created before the rock mass was drained in result of previous coal seam mining – probably shortly after the sinking of the shaft. The tests performed showed loose material forming in the lining around the void. In the roof of the void only scratches and cracks in the concrete indicate the occurrence of compact material.

Based on the data obtained, numerical model of the shaft lining with dimensions of 50 × 50 × 50 m was prepared (Fig. 6). The geological cross-section in the area of the voids encompasses a coarse sandstone, weakly compact, with a thickness of 41.5 m (68.5 to 110.0 m). Therefore, in the

numerical model a homogeneous rock mass with parameters shown in Table 2 was assumed.



Fig. 5. The void behind the shaft lining: a – the opening in the lining with dimension of approximately 0.05 × 0.10 m, b – the roof of the void with visible corrosion products

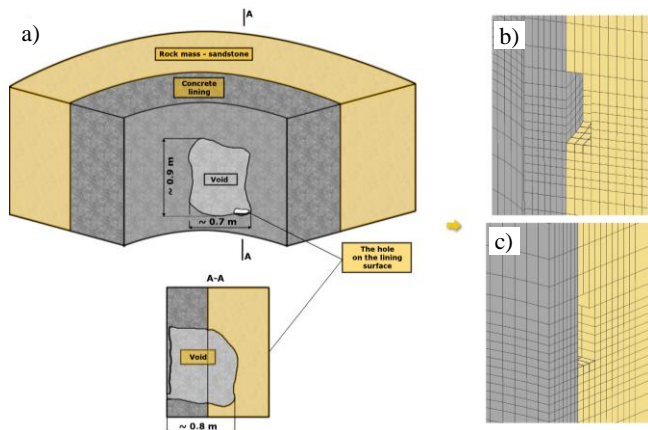


Fig. 6. The void in the tested area: a – sketch of the void based on the in situ tests, b – the numerical model of the void – view to the shaft, c – the numerical model of the void – view from the shaft

Table 2. Mechanical properties of the rock mass in the area of the void

Lithology	Intact rock UCS [MPa]	Density [kg/m ³]	Modulus of elasticity [MPa]	Rock mass Poisson's ratio [-]	Rock mass cohesion [MPa]	Internal friction angle [degree]	Rock mass tensile strength [MPa]	GSI [-]
Sandstone	24.0	2200	4500	0.23	4.30	25	0.55	50

Unfortunately, no strength tests of the concrete lining during the shaft inspection were carried out. Therefore, in the numerical calculations 5 variants of models with different parameters of the concrete lining were analysed (Table 3).

Table 3. Mechanical properties of the lining in the area of the void

Thickness [m]	UCS [MPa]	Density [kg/m ³]	Modulus of elasticity [MPa]	Poisson's ratio [-]	Cohesion [MPa]	Internal friction angle [degree]	Tensile strength [MPa]
0.5	15.0	2500	18,200	0.20	4.69	28	1.50
	10.0		14,900		3.12		1.00
	7.5		12,900		2.34		0.75
	5.0		10,500		1.56		0.50
	2.5		7,430		0.78		0.25

It was assumed that horizontal displacements at the side boundaries are equal to zero and vertical displacements at the bottom boundary also equal zero. At the top a load of 1.625 MPa was applied to represent the overburden of weight. The calculations were performed in stages:

- in the first stage the elastic model was solved,
- in the second stage the simulation of shaft sinking was simulated and the elastic-plastic model (C-M) was solved,
- in the third stage a stress-state in the lining was calculated,

- in the fourth step the appearance of the void was simulated and the changes in the stress-state of the lining were calculated.

Stages 2–4 were repeated for each subsequent types of concrete. The numerical calculations showed, that for concrete lining with a compressive strength of 15.0, 10.0 and 7.5 MPa the lining maintained its stability despite the presence of the void. This is mainly due to the small horizontal loads of the lining (about 0.9 MPa) resulting from the sandstone layer (Fig. 7).

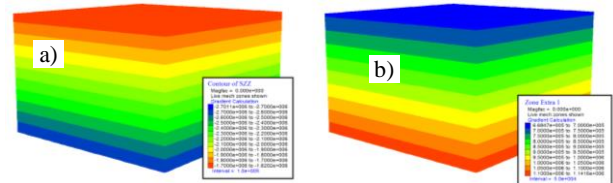


Fig. 7. Initial stress-state in the numerical model: a – the vertical stresses, b – the horizontal stresses

In the case of concrete lining with low compressive strength (2.5 MPa) the occurrence of void led to a wide gap in the lining and the destruction of an area of about 3.5 m² (Fig. 8). Among the studied variants of concrete strength the best results of numerical calculation were obtained for concrete with a compressive strength of 5 MPa (Fig. 9). The accuracy of the results was verified by the stress distribution in the lining and the occurrence of plasticity zones in the areas where the underground tests showed reduced compactness of concrete (loosened material).

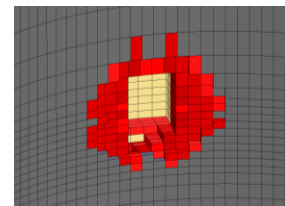


Fig. 8. Breach in the shaft lining in the area of void and the plasticity zone for low strength concrete lining (compressive strength equal 2.5 MPa)

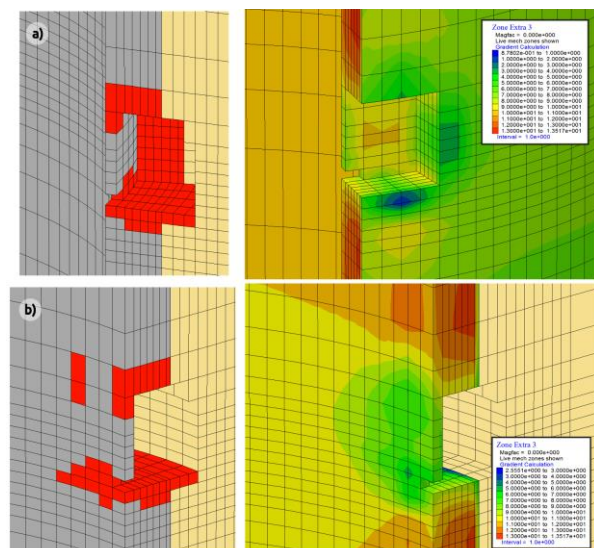


Fig. 9. Plasticity zone and strength factor of the lining for concrete with a compressive strength equal to 5 MPa: a – view to the shaft, b – view from the shaft

The results obtained from the numerical model of the void located in one of the shafts of the Upper Silesian Coal Basin allowed for the positive verification of the developed algorithm and methodology of the study. The numerical model obtained correctly mapped the distribution of stress in the lining and plasticity zone.

4. IMPACT OF VOID WITH VARIOUS VOLUME ON SHAFT STABILITY

The subroutine described above was used to analyse the impact of voids behind the shaft lining on shaft stability. Numerical analysis was carried out in stages. In the first stage, the model geometry was generated based on the initial parameters, and an elastic solution was calculated. In the next stage, the shaft was drilled, and the lining was erected. After solving the elastic-plastic model, additional sub-routines developed in the FISH language were used to create a matrix of the actual stress-displacement state and horizontal loading of the shaft lining. Finally, the growth of the void behind the lining was simulated, and the changes in the matrix were registered.

In addition, calculations were performed using the spalling subroutine described earlier. The adopted methodology is presented in diagram form in Figure 10, and a view of the generated model with total dimensions of 50 × 50 × 50 m is presented in Figure 11.

cases, the growth of the void behind the lining was simulated from step 0 (no voids behind the lining) to step 9 (Table 6, Fig. 12). In all models a constant shaft diameter (7.0 m) and Coulomb-Mohr failure criteria was assumed.

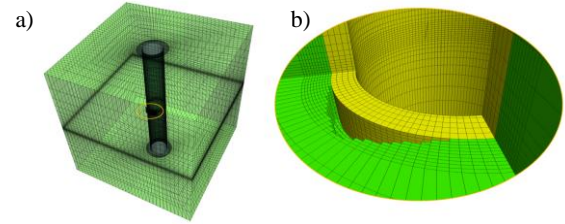


Fig. 11. Example of the numerical model used for computation: a – general view of the model, b – example of the simulated void behind the lining

Table 4. Mechanical properties of the rocks studied

Lithology	Intact rock UCS [MPa]	Density [kg/m³]	Modulus of elasticity [MPa]	Rock mass Poisson's ratio [-]	Rock mass cohesion [MPa]	Internal friction angle [degree]	Rock mass tensile strength [MPa]	GSI [-]
Shale stone	25.0	2300	6700	0.26	1.79	28	0.59	50
Coal	14.5	1300	2300	0.30	0.81	18	0.22	36
Sandstone	40.0	2400	11000	0.23	3.37	38	1.06	55

Table 5. Mechanical properties of the lining

Type (class) of concrete	Thickness [m]	UCS [MPa]	Density [kg/m³]	Modulus of elasticity [MPa]	Poisson's ratio [-]	Cohesion [MPa]	Internal friction angle [degree]	Tensile strength [MPa]
C12/15	0.3	15.0	2,500	18,200	0.20	4.69	28	1.50
	0.4							1.50
C16/20	0.5	20.0	2,500	21,000	0.20	6.25	28	2.00
	0.6							2.00
C20/25	0.7	25.0	2,500	23,500	0.20	7.81	28	2.50
	0.8							2.50
C25/30	0.9	30.0	2,500	25,700	0.20	9.37	28	3.00

Table 6. The subsequently growth of the void behind the lining

Calculation step	Maximum dimension of the void [m]	Void volume [m³]
1	0.5 × 0.3 × 0.1	0.014
2	1.0 × 0.6 × 0.2	0.076
3	1.5 × 0.9 × 0.3	0.203
4	2.0 × 1.2 × 0.4	0.476
5	2.5 × 1.5 × 0.5	0.894
6	3.0 × 1.8 × 0.6	1.438
7	3.5 × 2.1 × 0.7	2.252
8	4.0 × 2.4 × 0.8	3.072
9	4.5 × 2.7 × 0.9	4.489

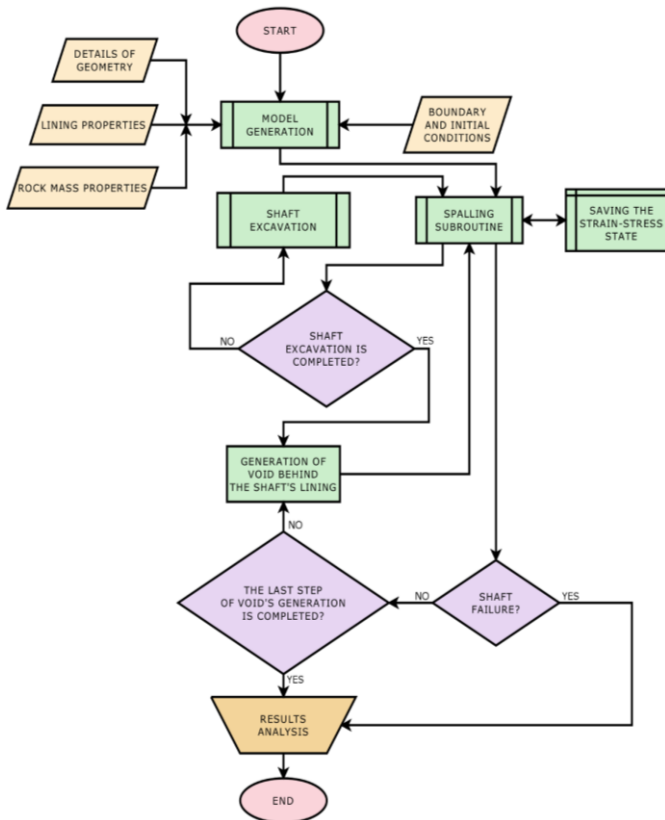


Fig. 10. Diagram of the adopted methodology

Numerical calculations were performed using three types of homogeneous rock mass commonly found in Poland in the Silesia Coal Basin (Bukowska, 2005): shale stone, coal, and sandstone. The mechanical properties of the rocks studied are shown in Table 4. In addition, variable lining strength parameters and thicknesses were analysed (Table 5). In each of the

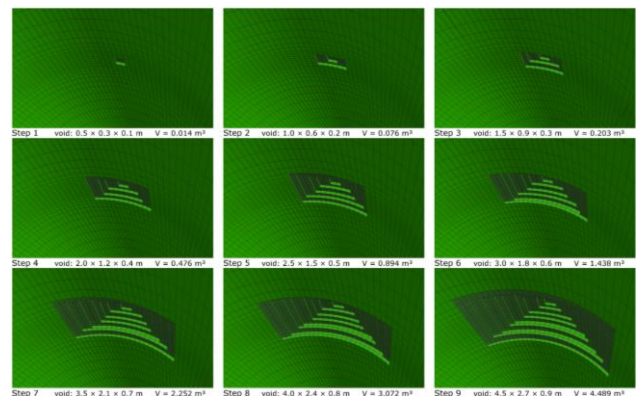


Fig. 12. Modelling of the void behind the lining in various stages

The use of the developed concrete spalling subroutine significantly influences the calculation results. Examples of the changes in the fracture zones and the loosening of the lining for the model with and without the subroutine are shown in Figure 13.

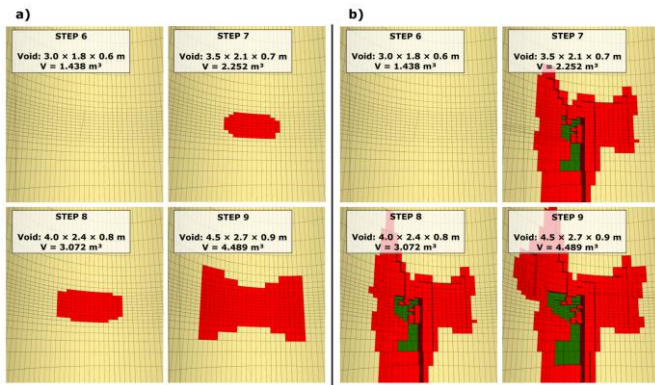


Fig. 13. Comparison of the calculated fracture zones and loosening of the lining for a void located in the shale stone at a depth of 600 m behind 50-cm-thick concrete lining (C20/25):
a – default model, b – model with spalling algorithm

The results presented in Figure 13 show that for the first steps of calculation in both models, the converging fracture zones were obtained. Differences began to emerge starting in step 7 (void with dimensions of $3.5 \times 2.1 \times 0.7$ m and a volume of 2.252 m^3). In the default model, only local fracture zones in the area of the void were observed. However, in the model with the spalling algorithm, the same void creates significantly larger fracture zones and more extensive loosening of the lining.

In the first stage of calculations aimed at the assessment of the impact of lining parameters on shaft stability in the area of voids, the following assumptions were made, there:

- was a homogeneous rock mass with parameters of shale stone,
- was a shaft diameter of 7 m,
- were two variants of the initial loading (10.0 and 15 MPa), corresponding to the presence of voids at depths of 400 and 600 m,
- were lining strength parameters corresponding to C12/15, C16/20, C20/25, and C25/30 concrete.

Figure 14 presents changes in the volume of the damaged lining for different types of concrete, various sizes of void and a constant thickness of the lining (0.3 m). The total volume of the damaged lining distinguished between three types of damage: fractured lining (where failure state of less than 50% of the tetrahedra comprising the zone was detected); destroyed lining (where more than 50% of the tetrahedra comprising the zone was damaged, but the destroyed zone was not removed from the model due to the previously described restrictions); and spalled lining (the zone was marked as destroyed; spalling simulation was executed).

Figure 15 presents the impact of various lining thickness and strength parameters on shaft stability in the area of the void with a constant volume of 4.5 m^3 . For reasons of clarity of the chart, the volume of the damaged lining wasn't distinguished between the three types of damage and only the total value was presented.

The first stage of calculations shows that in cases where the concrete class C12/C15 was used, regardless of the lining thickness, every emergence of a void created a loss of shaft stability. For lining with a thickness of 0.3 m, the critical void volume was equal to approximately 0.5 m^3 for C16/C20 concrete, approximately 0.9 m^3 for C20/C25 concrete, and ap-

proximately 1.5 m^3 for C25/C30 concrete. However, regardless of the class of concrete used for the lining, for thinner linings (0.3–0.5 m), a more dynamic impact of the void was observed. In turn, for thicker linings, regardless of the concrete class used, the increasing void behind the lining induced a slower, systematic expansion of the cracks in lining. Eventually, for some models, the concrete was destroyed and spalled, and the shaft became unstable.

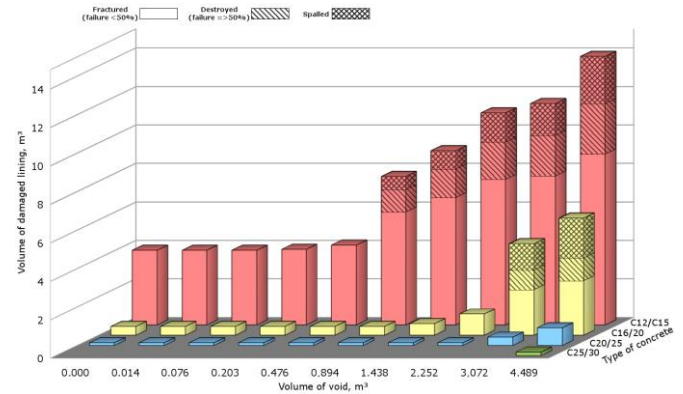


Fig. 14. Impact of lining strength parameters (thickness of 0.3 m) on shaft stability in the area of voids located at a depth of 400 m in shale stone

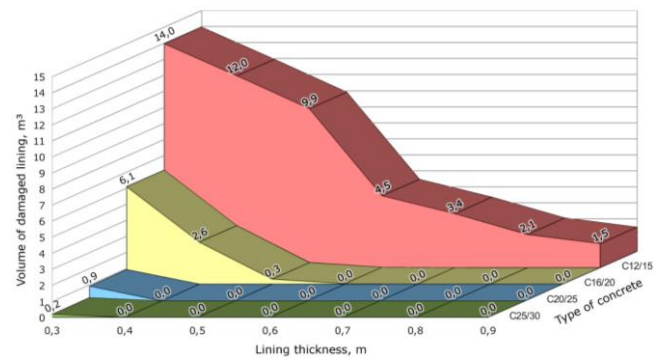


Fig. 15. Impact of lining thickness and strength parameters on shaft stability in the area of the void with a volume of 4.5 m^3 located at a depth of 400 m in shale stone

More dynamic changes were obtained for the models with an initial load corresponding to a depth of 600 m (Fig. 16 and 17).

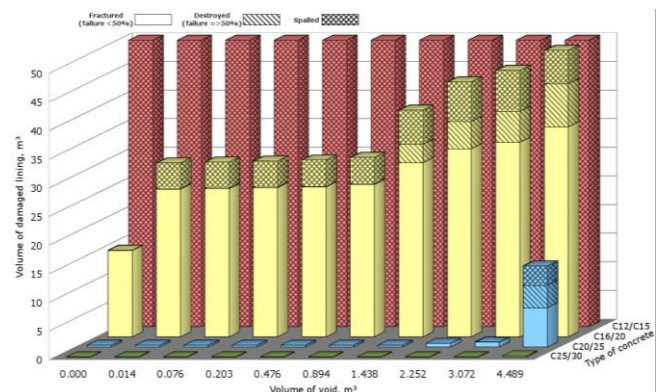


Fig. 16. Impact of lining strength parameters (thickness of 0.6 m) on shaft stability in the area of voids located at a depth of 600 m in shale stone

With the thusly altered initial conditions, regardless of the lining thickness or strength parameters, a relatively dynamic

impact of the void on the lining was observed, with a distinct increase in the fracture zone after exceeding the threshold values of the void. The limits varied for different models depending on the lining strength properties and thickness.

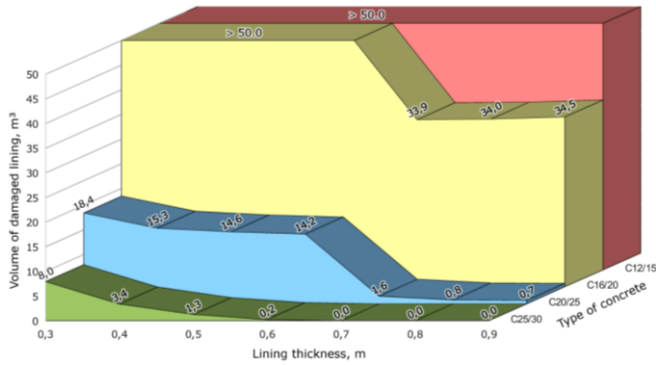


Fig. 17. Impact of lining thickness and strength parameters on shaft stability in the area of a 4.5-m³ void located at a depth of 600 m in shale stone

Of course, the shaft stability in the area of the void varies depending on the properties of the rock mass. Therefore, additional calculations were performed for the rock mass properties of coal. In most of the cases analysed, a loss of shaft stability was observed; in some of the models, this loss occurred even before the smallest void appeared. Only in cases of thick lining (0.8 and 0.9 m) of C25/30 concrete did the results show the possibility of preserving shaft stability without lining damage in the area of a 4.5-m³ void located at a depth of 400 m. Furthermore, the results indicate a significant increase in the dynamics of changes relative to the models with rock mass properties of shale stone (Fig. 18).

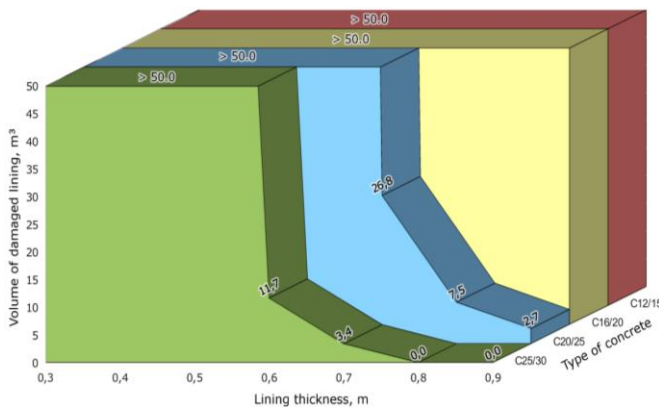


Fig. 18. Impact of lining thickness and strength parameters on shaft stability in the area of a 4.5-m³ void located at a depth of 400 m in coal

In the final stage of the calculations, a similar analysis was performed for the models with the rock mass properties of sandstone. The results show that the shaft remained stable, even for a 4.5-m³ void located at a depth of 400 m, regardless of the analysed lining thickness and strength parameters (only in the case of a 0.3-m-thick lining and lower strength parameters (C12/C15 concrete) was a small area of fractured and spalled concrete observed). A loss of shaft stability occurs only in cases of voids located at a depth of 600 m for lining made of low-strength concrete (Fig. 19).

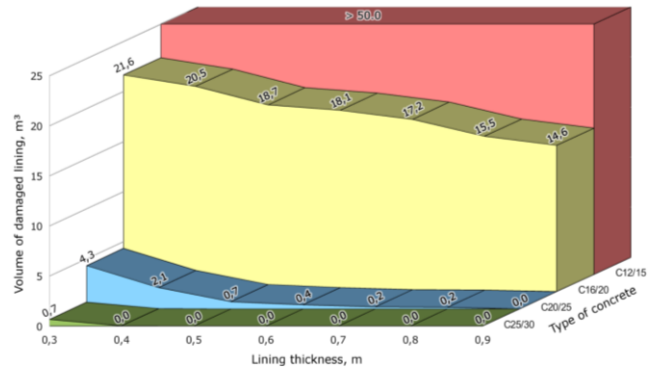


Fig. 19. Impact of lining thickness and strength parameters on shaft stability in the area of a 4.5-m³ void located at a depth of 600 m in sandstone

The results obtained also show that the sandstone model yielded less dynamic changes than the shale stone and coal models.

These examples only show some of the analysed cases; nevertheless, they are representative of the typical trends of the impact of voids on shaft stability for different conditions of their occurrence and lining parameters.

5. SUMMARY

Assessing the stability of existing concrete structures may require – as in the case of the lining of mine shafts – the inclusion of the identified lining damages in the calculations and the determination of their causes. To improve numerical analysis, a special algorithm has been developed and implemented in FLAC3D code using the built-in interpreter FISH. The algorithm extends the capabilities of FDM, thereby allowing the detachment and separation of destroyed lining fragments to be simulated. The comparative tests that obtained results for models with and without the spalling algorithm are similar for minor damages limited to a small area. Differences occur in cases of more extensive damage – the developed algorithm indicated the formation of areas of spalled concrete and increased the rate of structural deterioration in response.

This paper also presents an example of applications of the algorithm to evaluate the impact of voids behind the lining on shaft stability. The study included models using the rock mass properties of typical shale stone, coal, and sandstone found in the Upper Silesian Coal Basin. For each such variant, a series of calculations was performed for various lining thicknesses and strength properties and two initial loadings (corresponding to depths of 400 and 600 m). A total of 336 calculations of numerical models were performed. For each of the models, the impact of the gradual expansion of the void behind the lining on shaft stability was analysed. The results indicate that in most cases, the use of concrete with a higher compressive strength decreases void impact on shaft stability. However, this finding also causes an increase in the dynamics of the impact (e.g., an abrupt damage occurrence or loss of shaft stability). The dynamics of the changes were significantly influenced by the type of modelled rock mass; the growth of fractured zones was rapid for rock mass with coal properties, average for shale stone, and slow for sandstone.

Acknowledgements

The concrete spalling algorithm presented and the analysis of the impact of voids on the shaft lining were developed in the framework of the statutory activity: Analiza wpływu pustek za obudową szybową na jej stateczność metodą modelowania numerycznego (Analysis of the impact of voids on shaft lining using numerical modelling) – No. GIG: 13130211-153.

References

- Bock, S., Prusek, S., Rotkegel, M. (2009). Design and Control of Working Support in Polish Coal Mines Based on Three-Dimensional Numerical Modeling. In *28th International Conference on Ground Control in Mining* (pp. 113–120). Morgantown, W. VA: Dept. of Mining Engineering.
- Fakhimi, A., Salehi, D., Mojtabai, N. (2004). Numerical back analysis for estimation of soil parameters in the Resalat Tunnel project. *Tunnelling and Underground Space Technology*, 19(1), 57–67.
- FLAC3D v3.1: User Manual. Itasca Consulting Group, Minneapolis, MN, USA.
- Genis, M., Gercek, H. (2003). A numerical study of seismic damage to deep underground openings. In *International Society for Rock Mechanics, 10th Congress “Technology roadmap for Rock Mechanics”* (pp. 351–356). Marshalltown: The Southern African Institute of Mining and Metallurgy.
- Jing, L. (2003). A review of techniques, advances and outstanding issues in numerical modelling for rock mechanics and rock engineering. *International Journal of Rock Mechanics & Mining Sciences*, 40(3), 283–353.
- Karacan, C.Ö., Esterhuizen, G.S., Schatzel, S.J., Diamond, W.P. (2007). Reservoir simulation-based modeling for characterizing longwall methane emissions and gob gas venthole production. *International Journal of Coal Geology*, 71(2-3), 225–245.
- Lecomte, A., Salmon, R., Yang, W., Marshall, A., Purvis, M., Prusek, S., Bock, S., Gajda, L., Dziura, J., Niharra Munoz, A. (2012): Case studies and analysis of mine shafts incidents in Europe. In *3rd International Conference on Shaft Design and Construction, London 2012. Tunnels and Tunnelling International*, (1 May), 60–65.
- Prusek, S., Rotkegel, M., Bock, S., Szymała, J. (2011). Evaluation of technical state of mining shafts lining. *Schriftenreihe des Institutes für Geodäsie und der Technischen Universität Bergakademie Freiberg*, (2011-1), 201–209.
- Prusek S., Bock S., Uszko M., Dziura J. (2013). Selected methods for shaft lining repairs in Polish coal mines. In: *Conference Proceedings of 32rd World Mining Congress, Montreal, Canada*.
- Wisser, C., Augarde, C.E., Burd, H.J. (2005). Numerical modelling of compensation grouting above shallow tunnels. *International Journal for Numerical and Analytical Methods in Geomechanics*, 29(5), 443–471.